**GSA DATA REPOSITORY 2009232**

# Tsunami waves generated by the Santorini eruption reached Eastern Mediterranean shores

Beverly Goodman-Tchernov*, Hendrik Dey, Eduard Reinhardt, Floyd McCoy, and Yossi Mart

*E-mail: goodmanbeverly@gmail.com

This PDF file includes:
Methods: Collection and Processing
SOM Text
Figs. DR1 to DR7
Tables DR1 to DR3
References

## Methods: Core Collection and Processing

The cores were collected using an underwater pneumatic hammer attached by airhoses to a tending compressor at the surface and operated by divers below (Fig. DR1). Once drilled, the cores were capped and removed using air-lift bags. After collection, each core was photographed, described, and sampled at 1 cm intervals (unless sediment character required larger intervals), and subsampled for granulometry, micropaleontological analysis, and dating (Figs. DR2-DR6, Table DR1 and DR2). Chronological ages were based on (depending on availability in core) ceramics, OSL, and C14 (Tables DR1 and DR2). Granulometry was completed using Laser particle Analyzers (on a Beckman laser Coulter counter and Malvern Multisizer). Values from Malvern Multisizer varied from Beckman by a maximum of +/- 1%. Micropaleontological collection, analysis, and statistics were based on the methods of Fishbein and Patterson (*1*).

Foraminifera

The micropaleontology and sedimentology within the ancient harbor of Caesarea have been studied extensively (*2-4*). The Roman construction of the harbor walls (approximately 12 BCE) transitioned a high-energy open-water marine environment into a low-energy, organic-rich protected anchorage. Muds and silt predominated the ancient harbor floor, particularly while the harbor was in good repair. Those muds and silts within the harbor impacted the character of the foraminifera assemblage. Foraminifera

with higher tolerances for fine sediment and increased organic content were present in greater numbers than outside the harbor. Dominant species (*A. tepida* vs. *parkinsoniana*) were present in both the harbor phases and open water phases, but in inverse proportions (*2, 4*), unfortunately reducing their usefulness a useful nearshore/marine mixing indicator in the case of the mixed nearshore/marine tsunamigenic horizons. However, less-dominate but environmentally-significant foraminifera groups such as bolivinids were present within the harbor environment and absent otherwise. While in very low abundances, harbor taxa such as *Buccella* sp., *H. depressula, Bolivina* and *Brizalina* were present in the tsunamigenic horizons post-dating the harbor (Events 1 and 2, examples in Fig. DR1 and Fig. DR2 ), and were therefore useful as a microfossil indicator across cores. In some cases they were also present in the lower extent of the core, possibly reflecting different conditions, such as more developed estuaries, along the shoreline in periods predating the Roman Harbor. Presence/absence of these species were used in excavation trenchs, on muddy ripclasts, and through the core when full sample picking and identification was not carried out.

Archaeological Evidence

Within the cores and excavated trenches of this study, ceramics were present in the Event 1 and Event 2 horizons (Byzantine and Roman, respectively). Large pottery shards (>30cm) and heavy marble architectural fragments (>40cm blocks) were revealed in the Event 1 horizons. Smaller shards were found in the Event 2 horizon. One piece of non-diagnostic, heavily worn, and eroded pottery was found in association with Event 3.

Previous archaeological excavations within the Harbor of Caesarea reported a multitude of damage evidence contemporaneous with the periods of these events. The evidence includes discontinuous, patchy harbor floor muds, tilted massive (KE and KW towers, 5mX 5m) man-made marine structures, extensive underwater debris fields. Excavations in area W during this study, outside of the harbor, included clumps of mud, which are interpreted as muddy ripclasts that were eroded during the tsunami event from the harbor then transported into deeper waters during the return surge. Both the ripclasts and the presence of harbor-dwelling foraminifera taxa in the anomalous horizons suggest upper-shelf/nearshore mixing. Previous excavations were reassessed with regards to tsunami events and excavation reports were completed (*5, 6*).

Granulometry

Granulometry, (laser diffraction particle size distribution analysis) was completed using a Beckman–Coulter LS 230 (BC LS 230) laser and a Malvern Instruments Multisizer (M2500) and mathematical computations were completed using the Fraunhofer optical model. An aliquot of each sample was subsampled and digested with hydrogen peroxide to remove organics. Organics tend to get trapped on the lens of the reader and result in false measurements. While organics may also be a tsunamigenic indicator, in the case we chose to remove this variable to minimize machine-based error. Comparison of samples analyzed by the BC LS 230 versus the M2500 showed variation of no greater than 1% across distribution sizes, the M2500 producing more sensitive results. The proportions of each particle size bin were collected in an excel file and

exported into the Ocean Data View 3.3.2-2007 (http://odv.awi.de) for contour grid plotting on the scatter plot, VG gridding, X and Y scale length 30. The z-range (%) was limited to 10%.

Sediment description

The sediment description (Table DR3) can be summarized as follows (work completed by Floyd McCoy at American School in Athens). Sediments: 10 - 15% CaCO3; a few forams and ambiguous calcareous fragments that appear to be algal plates; and the typical mineralogic assortment of Nilotic sands and silts. Carbonate concentrations were done using the acid weight-loss method. Sediments were looked at using smear slides and a petrographic microscope. No fragments of tephra were found in the sediments attributed to tsunami deposition. This was not unexpected: tsunami would have arrived on the shores of the Levant within 60 - 100 minutes (Fig. DR1), whereas pumice rafts would have taken as much as 85-350 days to be transported to the Levant given contemporary surface current patterns and velocities (*7*). Given the trace quantities of volcanic ash particles found in Nile Delta sediments (*8*) it is clear that this area was at the periphery of the eruption plume and no significant amounts of ash would have been deposited here by air-fall mechanisms during, or following, the eruption, and thus contributed to offshore sediments.

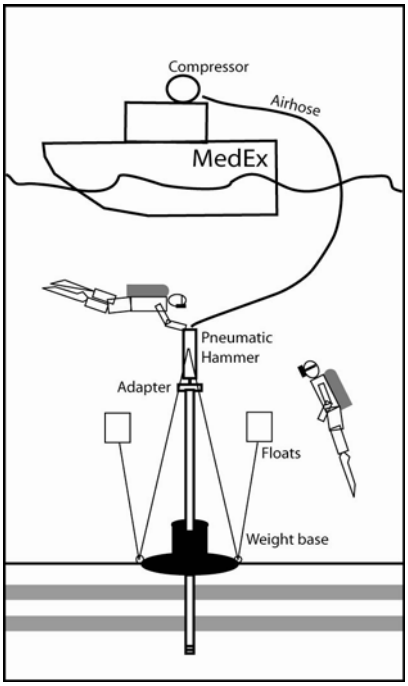


Figure DR1

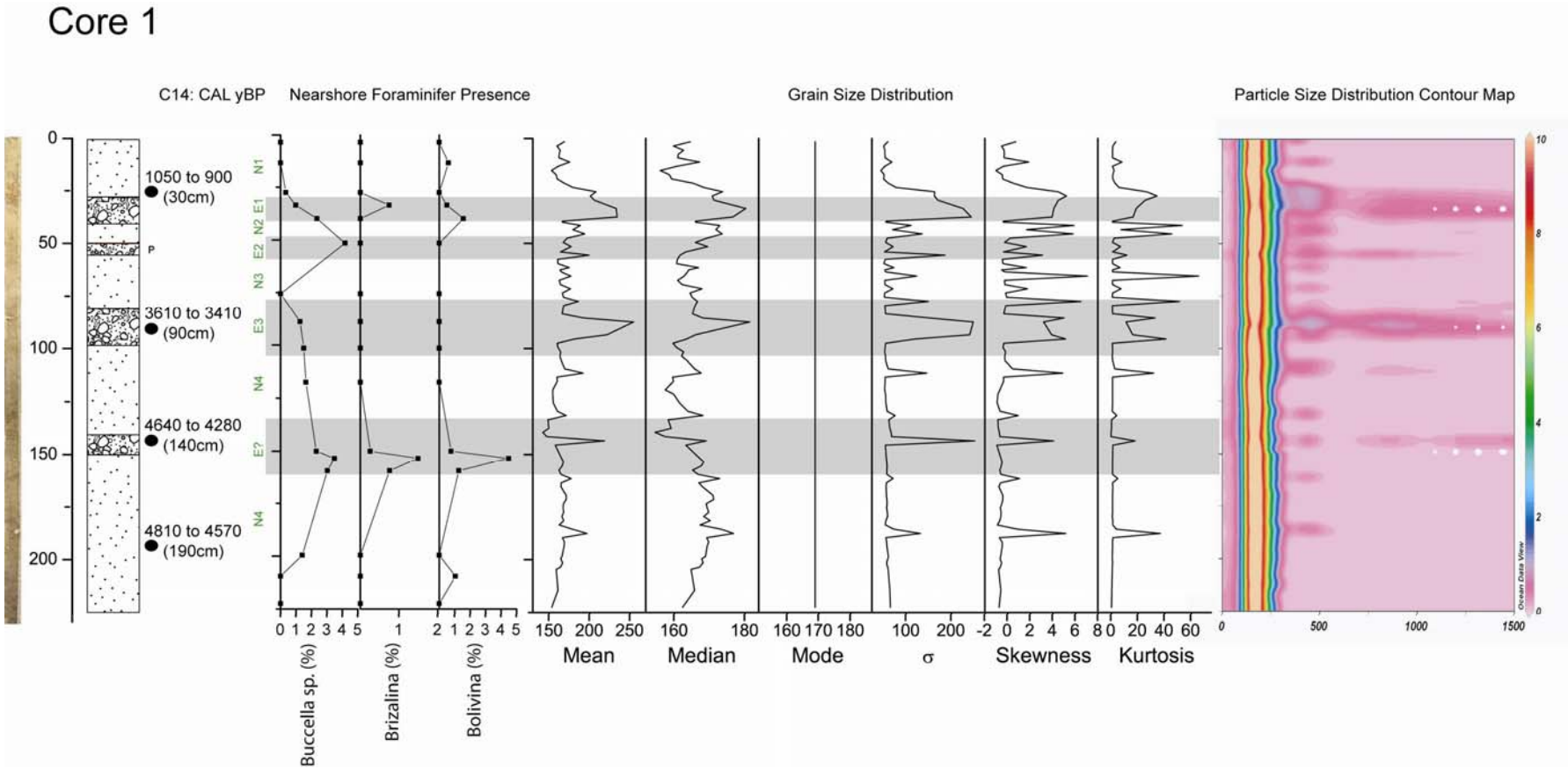
Core 1
C14: CAL yBP
Nearshore Foraminifer Presence
Grain Size Distribution
Particle Size Distribution Contour Map
1050 to 900 (30cm)
3610 to 3410 (90cm)
4640 to 4280 (140cm)
4810 to 4570 (190cm)
P
N1
E1
N2
E2
N3
E3
N4
E?
N4
Buccella sp. (%)
Brizalina (%)
Bolivina (%)
Mean
Median
Mode
σ
Skewness
Kurtosis

Figure DR2.

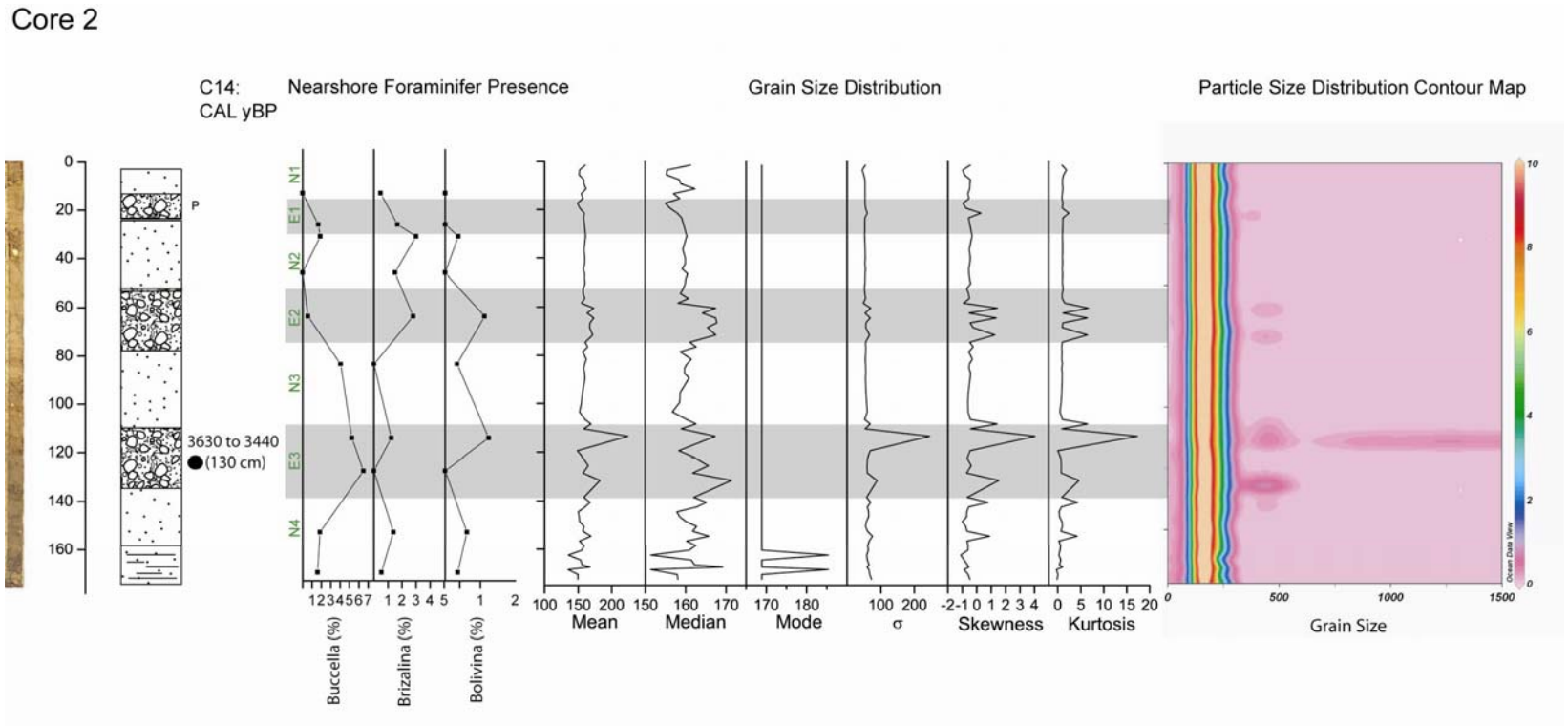
Core 2
C14:
CAL yBP
Nearshore Foraminifer Presence
Grain Size Distribution
Particle Size Distribution Contour Map
0
20
40
60
80
100
120
140
160
P
3630 to 3440
(130 cm)
N1
E1
N2
E2
N3
E3
N4
1 2 3 4 5 6 7
1 2 3 4 5
1
2
Buccella (%)
Brizalina (%)
Bolivina (%)
100 150 200
Mean
150 160 170
Median
170 180
Mode
100 200
σ
-2 -1 0 1 2 3 4
Skewness
0 5 10 15 20
Kurtosis
0
500
1000
1500
Grain Size
10
8
6
4
2
0
Ocean Data View

Figure DR3.

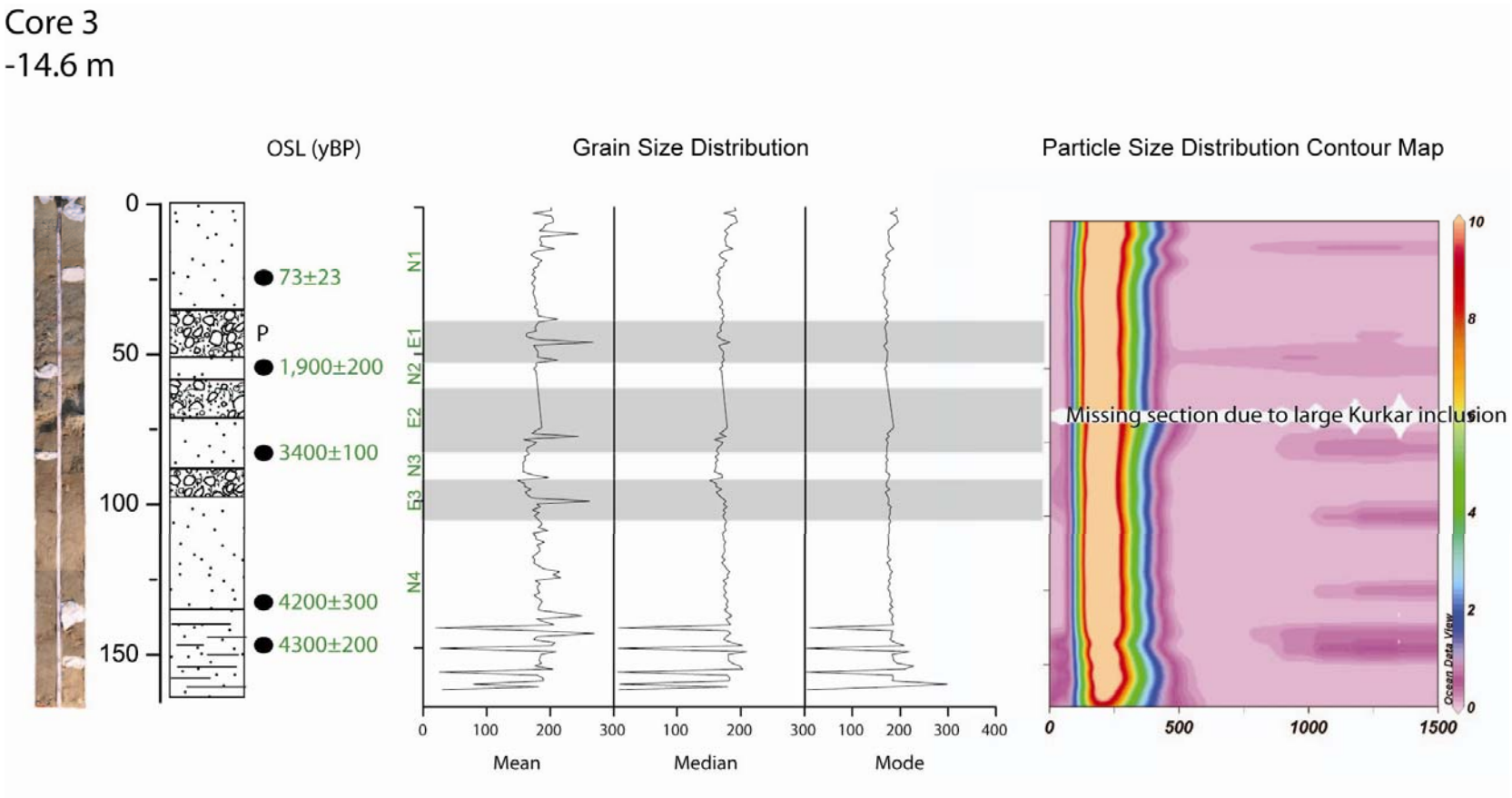
Core 3
-14.6 m
OSL (yBP)
Grain Size Distribution
Particle Size Distribution Contour Map
0
50
100
150
73±23
P
1,900±200
3400±100
4200±300
4300±200
N1
E1
N2
E2
N3
E3
N4
0
100
200
300
100
200
300
100
200
300
400
Mean
Median
Mode
Missing section due to large Kurkar inclusion
0
500
1000
1500
10
8
4
2
0
Ocean Data View

Figure DR4.

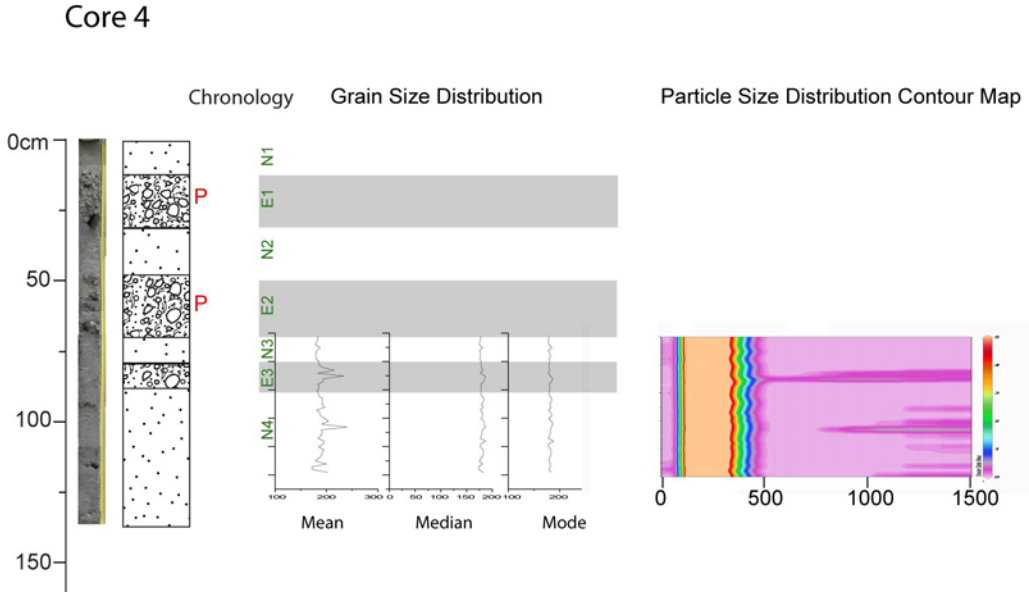
Core 4
Chronology
Grain Size Distribution
Particle Size Distribution Contour Map
0cm
50
100
150
P
P
N1
E1
N2
E2
N3
E3
N4
Mean
Median
Mode
0
500
1000
1500

Figure DR5.

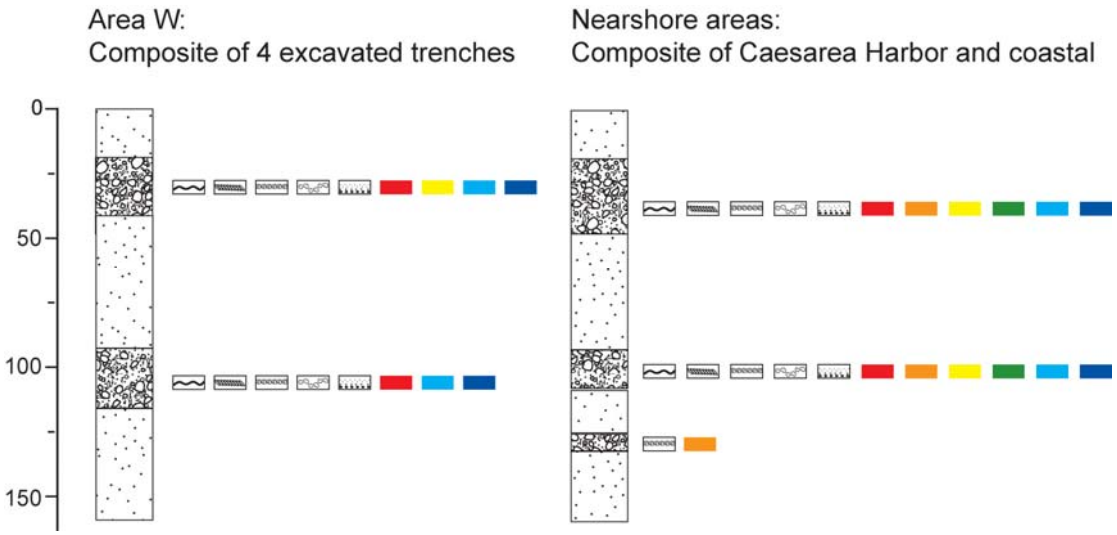
Area W:
Composite of 4 excavated trenches
Nearshore areas:
Composite of Caesarea Harbor and coastal
0
50
100
150

Figure DR6

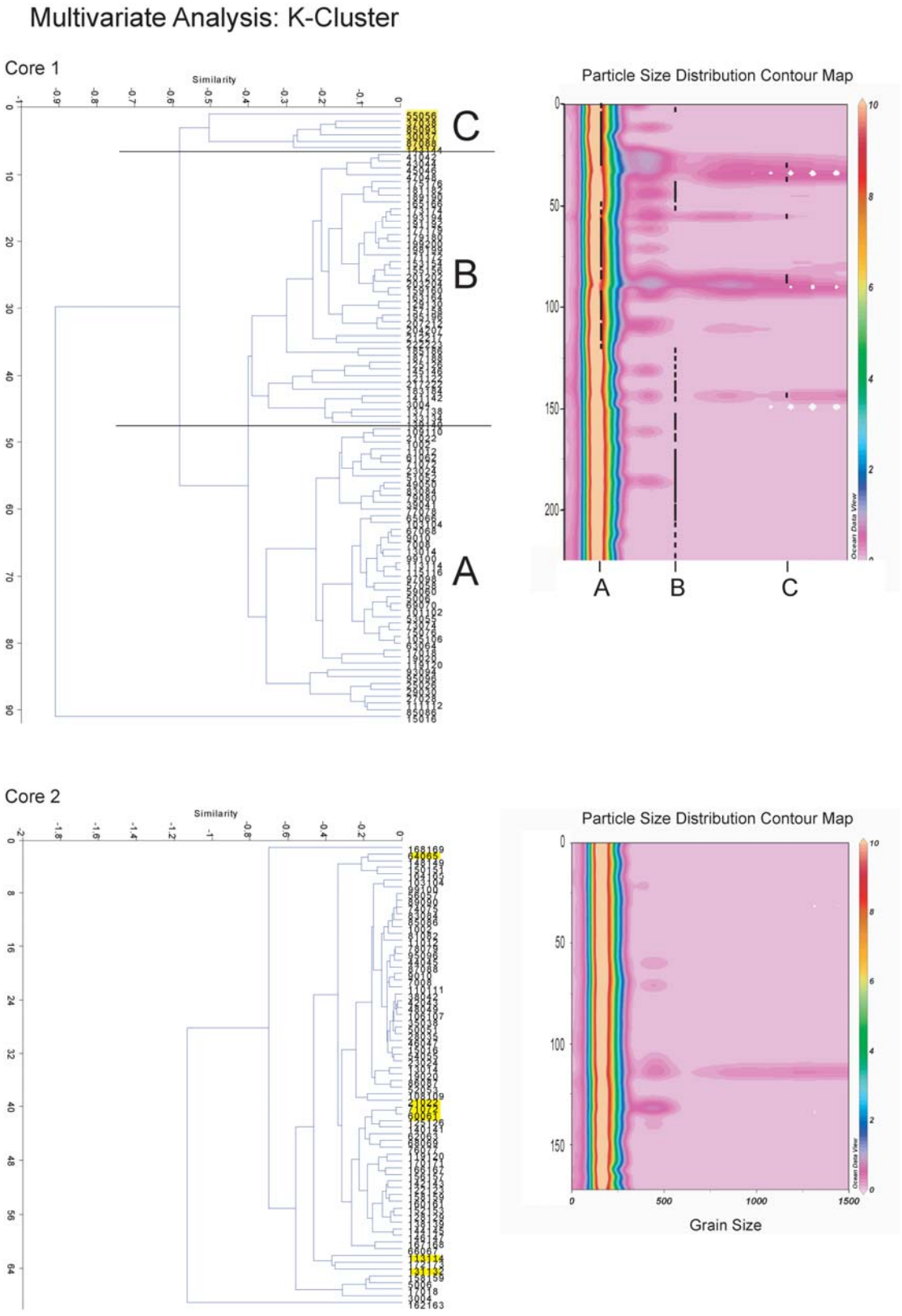
Multivariate Analysis: K-Cluster
Core 1
Similarity
C
B
A
Particle Size Distribution Contour Map
A
B
C
Core 2
Similarity
Particle Size Distribution Contour Map
Grain Size

Figure DR7

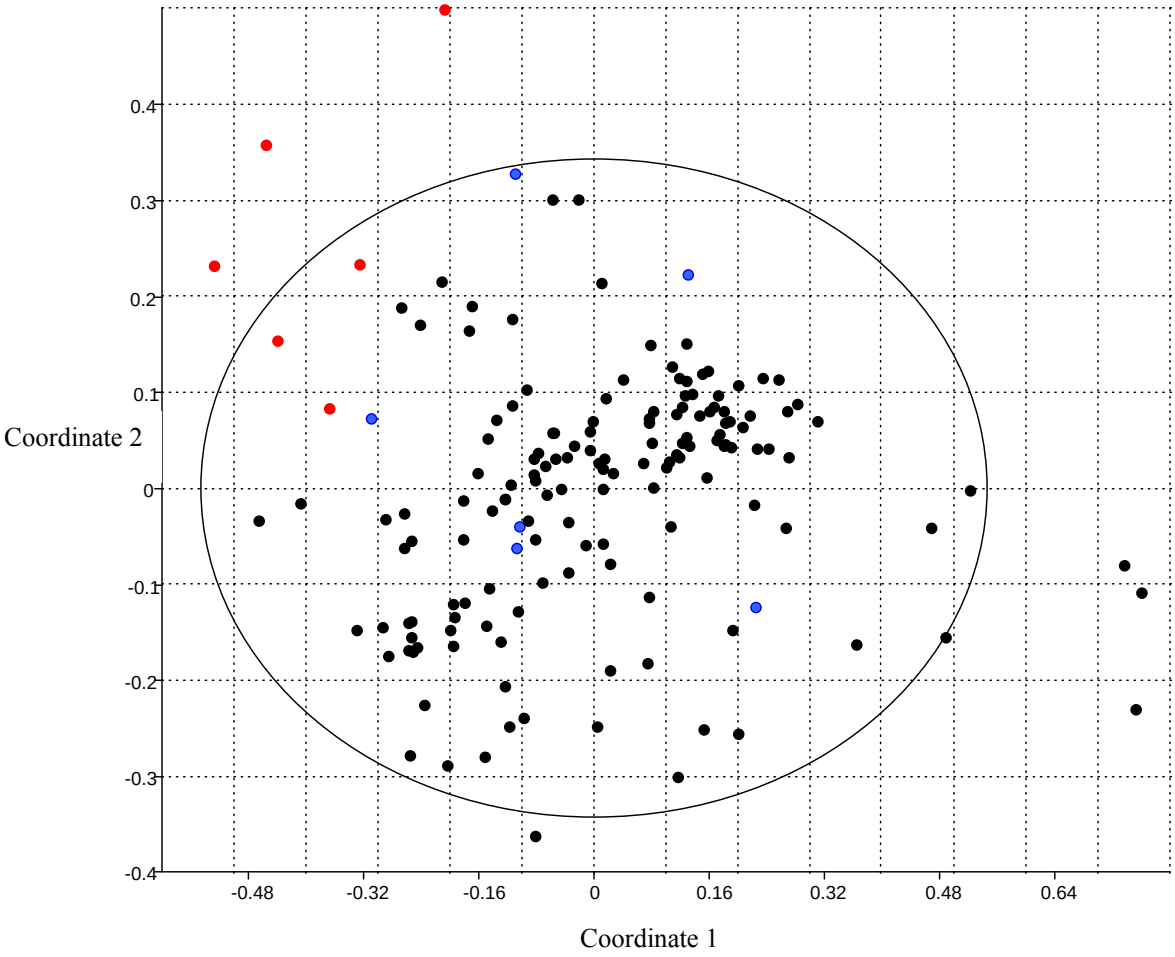


Fig DR8

**CAPTIONS**

Fig. DR1. LEXY coring procedure illustrated. An aluminum pipe fitted with a brass core catcher is hammered into the seabed with a pneumatic hammer. Floats attached to the hammer and through a base weight balance the core and provide additional downward force for the hammering. The compressed air is provided from a compressor placed on the tending work platform, in this case the research ship the Mediterranean Explorer. The core is then removed using floats.

Fig. DR2. Sample of Results of core analysis, Core 1. N=Normal conditions interevent, followed by the number in the sequence (1-4) and E=Tsunami event, followed by number in sequence (1-3). E? indicates horizon that fits many tsunamigenic criteria, but was not areally extensive, and thus was not considered as a candidate in the study.

Figure DR3. Results of core analysis, Core 2. N=Normal conditions interevent, followed by the number in the sequence (1-4) and E=Tsunami event, followed by number in

sequence (1-3). P= dateable ceramics present in horizon (in agreement with age range unless noted).

Figure DR4. Results of core analysis, Core 3. N=Normal conditions interevent, followed by the number in the sequence (1-4) and E=Tsunami event, followed by number in sequence (1-3). P= dateable ceramics present in horizon (in agreement with age range unless noted). Large gap in contour map is due to kurkar (local bedrock) inclusion. White sections in photograph indicate sections where OSL samples were collected.

Figure DR5. Results of core analysis, Core 3. N=Normal conditions interevent, followed by the number in the sequence (1-4) and E=Tsunami event, followed by number in sequence (1-3). P= dateable ceramics present in horizon (in agreement with age range unless noted). Particle size results completed in lower section (70 to 120cm) only.

Figure DR6. Summary of tsunamic characteristics identified in area W and Terrestrial and Nearshore from this and previous studies (*2-4, 6, 9*)*).* The nearshore areas, in this representation, have included Tel Aviv area evidence (*10, 11*).

Fig. DR7. Multivariate analysis K-clustering of particle distribution results, completed using PAST software (*12-14*). Core 1 demonstrates that the tsunamigenic horizon samples cluster together ('A'), while the remaining samples cluster into two ('B' and 'C') categories that represent both designated storm layers and normal marine conditions. This illustrates the stronger variation between the tsunami events versus normal conditions as compared to storm events versus normal conditions. Storms are wind-driven and represent an increase in wave energy, while the mechanistic source of tsunami-waves is disturbance driven (underwater slumping, tectonics, volcanic eruptions, etc.), which may account for this difference. Tsunamigenic horizons have been highlighted in yellow in both cluster diagrams.

Table DR1.

| Core/Area # | Depth in Section (cm) | Analysis | 13C/12C Ratio o/oo | Conventional Radiocarbon (BP) | 2 sigma calibration | Event | Reference |
|---|---|---|---|---|---|---|---|
| 1 | 30 | AMS | +2.7 | 1420 ± 40 | Cal AD 900 to 1050 (Cal BP 1050 to 900) | post-E2 | This study |
| 1 | 90 | AMS | +3.0 | 3610 ± 40 | Cal BC 1660 to 1460 (Cal BP 3610 to 3410) | E3 | This study |
| 1 | 140 | Radiometric | +0.8 | 4330 ± 70 | Cal BC 2700 to 2330 (Cal BP 4640 to 4280) | N/A | This study |
| 1 | 190 | AMS | +2.7 | 4500 ± 40 | Cal BC 2860 to 2620 (Cal BP 4810 to 4570) | N/A | This study |
| 2 | 130 | AMS | +2.2 | 3640 ± 40 | Cal BC 1680 to 1490 (Cal BP 3630 to 3440) | E3 | This study |
| W | 12.3 | Radiometric | +1.3 | 2330 ± 100 | Cal BC 364 to Cal AD 218 (Cal BP 1732 to 2314) | NC2 | (*9*) |
| W | 12.6 | Radiometric | +1.0 | 2310 ± 80 | Cal BC 350 to Cal AD 226 (Cal BP 2300 to 1724) | E2 | (*9*) |

Table DR2.

| Core#/Area | Horizon | Depth (cm) | Ext. g (mGy/a) | Cosmic (mGy/a) | K % | U (ppm) *0.01 | Th (ppm) | Ext. b (mGy/a) | Total dose (mGy/a) | No. of discs | De (Gy) | Age (ka) | Calendar Date | Range | Lab | Reference |
|---|---|---|---|---|---|---|---|---|---|---|---|---|---|---|---|---|
| 3 | N1 | 23-26 | 322 | 87 | 0.62 | 1.2 | 2.3 | 512 | 924±35 | 12/12 | 0.07±0.02 | *0.73±0.23* | 1935 AD | 1912-1958AD | GSI | this study |
| 3 | E2 | 55-58 | 268 | 84 | 0.61 | 1.1 | 1.2 | 475 | 830±33 | 11/12 | 1.6±0.1 | 1.9±0.2 | 108 AD | 92 BC-308AD | GSI | this study |
| 3 | N3 | 81.5-84.5 | 323 | 82 | 0.58 | 1.5 | 1.8 | 511 | 919±35 | 6/12 | 3.13±0.06 | 3.4±0.1 | 1392 BC | 1492-1292 BC | GSI | this study |
| 3 | N4 | 133.5-137.5 | 283 | 78 | 0.53 | 1.3 | 1.5 | 457 | 821±32 | 11/12 | 3.5±0.2 | 4.2±0.3 | 2192 BC | 2492-1892BC | GSI | this study |
| 3 | N4 | 149.5-153.5 | 303 | 77 | 0.51 | 1.4 | 1.9 | 464 | 847±33 | 11/12 | 3.6±0.15 | 4.3±0.2 | 2292 BC | 2492-2092 BC | GSI | this study |
| W | N2 | 12.7 | | 96 | 0.7095± 0.02 | 0.71* | 0.79± 0.07 | | 778.4± 14.6 | | 1.46±0.12 | | 130 AD | 69 BC - 329 AD | MU | (*9*) |
| W | N2 | 11.6 | | 93 | 0.6420± 0.02 | 0.57* | 0.82±0.08 | | 704.2± 11.9 | | 1.42±0.13 | | 11 BC | 238 BC-216 AD | MU | (*9*) |
| W | N4 | 12 | | 89 | 0.4296± 0.01 | 1.07* | 1.13±0.05 | | 689± 14.8 | | 3.28±0.14 | | 2754 BC | 3133-2375 BC | MU | (*9*) |
| (*9*)W | N4 | 12.5 | | 83 | 0.5309± 0.02 | 1.17* | 1.37±0.10 | | 779.1± 18.1 | | 3.44±0.14 | | 2410 BC | 2764-2056 BC | MU | (*9*) |

## Geological Survey of Israel (GSI) lab comments:

Quartz samples, grain size 125-177 μm. All samples were etched by concentrated HF for 40 minutes. De was obtained using the single aliquot regeneration (SAR) protocol (*15*), with preheats of 10s @ 220-260°C and cutheats of 5s @ 20° below preheat. No. of discs is the number from those measured that was used for calculating the De. Dose rates were calculated from the concentrations of the radioactive elements U, Th and K, (measured by ICP-MS or ICP AES) and the contribution of the cosmic dose. External alpha dose is 2-3 mGy/a (not in Table). Water contents were estimated at 20%, based on laboratory measurements and assuming some sample drying. The shielding affect for cosmic dose calculation takes into account the sediment cover (core depth) and the water depth of the core. Ages are before 2008.
Technician: Michael Davis, March 2008

## McMaster University (MU) lab comments:

De was determined using the single-aliquot regnerative-dose (SAR) protocol (17). U, Th, and K values were determined by NAA. Cosmic ray dose rate value was calculated using an average density model for the overburden (water column + sediment thickness). Corrected laboratory water content accounting for water content geometry and sediment compaction during coring. All γ and β rates were calculated based on U, Th, and K concentrations of each sample accounting for moisture values of the sample. Internal concentrations of $^{238}$ U and $^{232}$ Th were used based on Rink and Odom (1991) (*16*) calculations for granitic quartz. Datum for SAR-OSL ages is A.D. 2005 and error is 1. Ages were calculated assuming rapid sediment accumulation (i.e. true sample depth below MSL)

Table DR3

| Bag Label | Sample Code | Horizon |
|---|---|---|
| Caesarea, Core 2, 130cm | CT2130135 | Event 3:Santorini |
| Caesarea, Core 2, 120cm | CT2120125 | Event 3:Santorini |
| Caesarea, Core 1, 90cm | CT1090095 | Event 3:Santorini |
| Caesarea, Core 3, 92-93cm | CT3092093 | Event 3: Santorini |
| Caesarea, Core1, 18-19cm | CT1018019 | Normal marine (NC1) |
| Caesarea, Core 2, 10cm | CT2010015 | Normal marine (NC1) |

.

## TABLE CAPTIONS

Table DR1.
Supplement Table 1. Radiocarbon-14 results from this study. Horizon designations N=Normal conditions interevent, followed by the number in the sequence (1-4) and E=Tsunami event, followed by number in sequence (1-3). All dates calibrated using database MARINE04, INTCAL04 Radiocarbon Age Calibration (*17*) and mathematics provided by Talma and Vogel 1993(*18*). The radiocarbon-14 ages were calibrated to calendar years in accordance with Reiner et al. (2004) and Stuiver and Braziunas (1993) (*19, 20*). Dates from previous study (9) were recalibrated with the updated calibration curves. Additional radiocarbon dates from archaeological reports which are applicable to terrestrial and nearshore positions reports are available in excavation reports (*6*).

Table DR2.
OSL ages. Horizon designations N=Normal conditions interevent, followed by the number in the sequence (1-4) and E=Tsunami event, followed by number in sequence (1-3). Optically stimulated luminescence (OSL) ages reported from IGS= N. Porat, Israel Geological Survey, Jerusalem and MU=McMaster University, Hamilton, Ontario.

## REFERENCES CITED


1. E. Fishbein, R. T. Patterson, *Journal of Paleontology* **67**, 475 (1993).
2. E. G. Reinhardt, Patterson, R.T., and Schröder-Adams, C., *Journal of Foraminiferal Research* **24**, 37 (1994).
3. E. G. Reinhardt, R.T. Patterson, J. Blenkinsop, and A. Raban, *Revue de paleobiologie*, 1 (1998).
4. E. G. Reinhardt, Raban, A., *Geology* **27**, 811 (1999).
5. E. G. Reinhardt, and Raban, A., in *Caesarea Reports and Studies: Excavations within the Old City and the Harbor 1996-2007, British Archaeological Reports, International Series, no. 1784* S. K. Holum, J., Reinhardt, E., Ed. (University of Michigan Press, Ann Arbor, 2008).
6. A. Raban, in *Caesarea Reports and Studies: Excavations within the Old City and the Harbor 1996-2007, British Archaeological Reports, International Series, no. 1784* S. K. Holum, J., Reinhardt, E., Ed. (University of Michigan Press, Ann Arbor, 2008).
7. F. McCoy, and Heiken, G., *Pure Applied Geophysics* **157**, 1227 (2000).
8. D. J. Stanley, H. Sheng, *Nature* **320**, 733 (1986).
9. E. G. Reinhardt *et al.*, *Geology* **34**, 1061 (2006).
10. D. Neev, Bakler, N., and Emery, K. O., *Mediterranean Coasts of Israel and Sinai* (Taylor and Francis, New York, 1987), pp. 130.
11. M. Pfannenstiel, *Bull. Instit. Oceanographique* **1192** (1960).

12. Ø. Hammer, Harper, D.A.T., and P. D. Ryan, *Palaeontologia Electronica* **4**, http://palaeo (2001).
13. J. I. Boyce, E. G. Reinhardt, B. N. Goodman, *Journal of Archaeological Science* **36**, 1516 (2009).
14. S. V. Donato, E. G. Reinhardt, J. I. Boyce, R. Rothaus, T. Vosmer, *Geology* **36**, 199 (2008).
15. A. S. Murray, A. G. Wintle, *Radiation Measurements* **32**, 57 (2000).
16. W. J. Rink, Odom, A. L., *Nuclear Tracks Radiation Measurements* **18**, 163 (1991).
17. M. Stuiver, Reimer, P.J., Bard, E., Beck, J.W., Burr, G.S., Hughen, K.A., Kromer, M. B., F.G., v.d.Plicht, J., and Spurk, M., *Radiocarbon* **40**, 1041–1083 (1998).
18. A. S. Talma, Vogel, J.C., *Radiocarbon* **35**, 317 (1993).
19. P. J. Reimer, and McCormac, F.G., *Radiocarbon* **44**, 159–166 (2002).
20. M. Stuiver, and Reimer, P.J., *Radiocarbon* **13**, 215 (1993).